Formation of island chains in SiGe/Si heteroepitaxy by elastic anisotropy

M. Meixner and E. Schöll

Institut für Theoretische Physik, Technische Universität Berlin, Hardenbergstrasse 36, D-10623 Berlin, Germany

M. Schmidbauer, H. Raidt, and R. Köhler

AG Röntgenbeugung, Institut für Physik, Humboldt-Universität zu Berlin, Hausvogteiplatz 5-7, D-10117 Berlin, Germany

In LPE-grown semiconductor samples the formation of self-assembled nanoscale island chains along the elastically soft $\langle 100 \rangle$ directions can be observed. We explain this process of self-organization by a kinetic Monte Carlo simulation of the Stranski-Krastanow growth mode, incorporating in a self-consistent way the anisotropic strain field around the nanoscale islands.

I. INTRODUCTION

Semiconductor nanostructures are currently of great interest with regard to the fabrication of high-performance optoelectronic devices.[1] In materials exhibiting a sufficiently large lattice mismatch, nanoscale islands [quantum dots, (QD's)] can be generated during heteroepitaxy by utilizing self-assembling mechanisms such as the Stranski-Krastanow growth mode.[2] The evolution of QD's is often accompanied by strong positional correlation effects.[3–5] Lateral correlation can be present within a single layer of QD's, but vertical correlation or anticorrelation is also observed in multifold stacked systems, provided that the spacer layers separating the QD's are thin enough. The latter case indicates the significance of strain for the self-organized formation of nanoscale islands.

Though most of the early theoretical work is based on energy considerations,[6–8] the influence of kinetic effects during growth has turned out to be very crucial. Those kinetic limitations play a central role for a detailed understanding of the island growth, and they strongly depend on the growth conditions. Recent studies[9,10] have shown that a kinetic energy barrier for growth on the island facets can lead to self-limiting growth.

The aim of this paper is to help to deepen our understanding of self-organized island growth by comparing experimental results obtained in liquid phase epitaxy (LPE) grown $Si_{1-x}Ge_x/Si(001)$ islands with kinetic Monte Carlo (KMC) simulations. In particular we show that the formation of chains of two or more islands along $\langle 100 \rangle$ directions under certain growth conditions can be explained by the interplay of kinetics with the anisotropic strain field that is generated by the islands. As compared to well known growth techniques such as molecular beam epitaxy (MBE) or metal organic chemical vapor deposition (MOCVD) LPE is carried out rather close to thermodynamic equilibrium.[11] A metal melt (e.g., Bi or In) containing, e.g., Si and/or Ge is put onto a Si substrate and cooled down such that epitaxial growth occurs via oversaturation of the melt. A more detailed description of the growth procedure is given elsewhere.[12] As a consequence of conditions close to equilibrium highly regular, facetted, coherent $Si_{1-x}Ge_x$ truncated pyramids with a narrow size distribution are grown on Si(001). It has been

shown that the island size is independent of the growth rate and growth temperature but is given by a simple scaling behavior between the island base width and the Ge concentration (and thus the lattice mismatch).[13]

At sufficiently high island densities a high degree of positional correlation is observed. Dorsch *et al.*[14] attribute this to an underlying ripple pattern aligned along $\langle 100 \rangle$ that—at later stages of growth—transforms into three-dimensional (3D) islands. The corresponding distances between islands are, therefore, determined by the wavelength of the underlying ripple pattern. Such a pattern is only observed at low ($x < 0.15$) Ge content. Positional correlation is observed, however, also in the case of an absent ripple pattern ($x > 0.15$).

II. EXPERIMENTAL RESULTS

The following observations indicate a significant influence of strain upon growth kinetics. At low island coverage, i.e., large mean island-island distances, island "dimers" and "trimers," i.e., chains of two or three islands, are formed[12] [Fig. 1(a)]. By increasing the island coverage during growth these linear clusters develop into extended chains along the $\langle 100 \rangle$ directions [Fig. 2(a)]. This obviously implies an aniso-
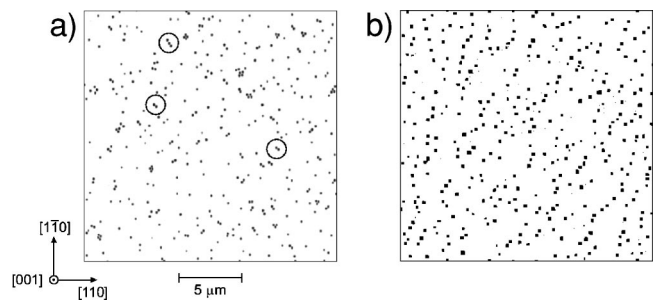

FIG. 1. (a) Atomic force micrographs (AFM) picture of LPE grown $Si_{0.75}Ge_{0.25}/Si(001)$ islands at low coverage (submonolayer coverge $c = 0.02$, excluding the wetting layer). There is a high percentage of islands (of width 150 nm and height 90 nm) arranged in dimers and trimers oriented along $\langle 100 \rangle$ (e.g., marked by circles). (b) Results of the kinetic Monte Carlo simulation ($T = 650$ K, growth rate 0.01 ML/s; coverage $c = 0.05$, after 200 s growth interruption).
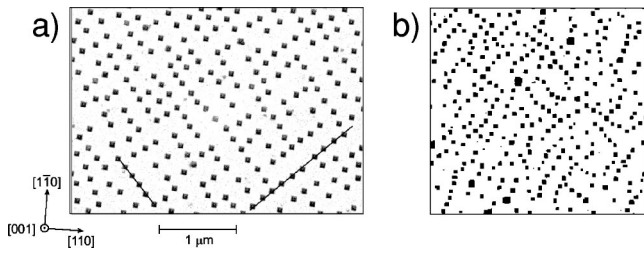
FIG. 2. (a) Formation of linear $Si_{0.75}Ge_{0.25}$ island chains along $\langle 100 \rangle$ at higher coverage $c = 0.16$ (scanning electron micrograph). Comparison of the island distance within closely spaced chains (see, e.g., those two marked by lines) and the chain-chain distance exhibits a significant difference, which indicates an independent development of the chains during growth. (b) Results of the kinetic Monte Carlo simulation ($T = 650$ K, growth rate 0.01 ML/s; coverage $c = 0.2$, after 200 s growth interruption).

tropic (inhomogeneous) probability of island formation around an already existing island. This is supported by depletion of the wetting layer in the immediate environment of the islands as reported, e.g., in Ref. 15. However, our observations further show that the depletion is closely related to the strain energy distribution around an island. This is demonstrated in Fig. 3, where a reduced thickness of the wetting layer around fully developed islands can be observed. The depletion looks similar to the elastic strain energy distribution [Fig. 4(a)], i.e., the wetting layer is partly removed at areas of high strain energy. The reduced wetting layer thickness and the considerable strain concentration at the island edges seem to prevent nucleation at $\{111\}$ facets from the wetting layer. Two-dimensional nucleation on $\{111\}$ surfaces is rather unfavorable in case of LPE growth.

We would like to emphasize that depletion is observed only for rather large islands (as depicted in Fig. 3), i.e., at low Ge content ($x < 15\%$), and it is in the range of a few nanometers. At higher Ge content [$x = 25\%$, Figs. 1(a), 2(a)] a significant depletion of the wetting layer has not been detected so far. Our strain calculations do not yet take into account the wetting layer depletion. We expect that this will lead to areas of reduced strain energy (as compared to an
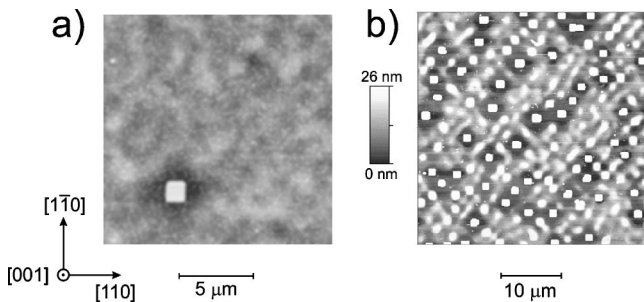

FIG. 4. (a) Numerical finite element calculation of the strain energy density for a facetted truncated pyramid of $Si_{0.75}Ge_{0.25}$. The energy density at the substrate-island interface is displayed. The island contours are shown in black. The greyscale varies from low values of strain energy density (dark) to high values (bright). (b) Calculated anisotropic strain energy density $E_{str}(x,y)$ [using Eq. (3)] of a circular $Si_{0.75}Ge_{0.25}$ 2D island in the (001) plane for elastic moduli $c_{11} = 1.58 \times 10^{12}$ erg/cm^3, $c_{12} = 0.60 \times 10^{12}$ erg/cm^3 and $c_{44} = 0.77 \times 10^{12}$ erg/cm^3 (linear interpolation of the bulk values of Si and Ge). The inset shows the strain energy profile of a cut along the line in $\langle 110 \rangle$ direction in a logarithmic scale (arbitrary units).

extended wetting layer), and will thus favor nucleation between areas of depletion.

The combined strain field of two adjacent islands (*dimer*) increases the strain energy perpendicular to their connection line. Therefore, favored nucleation sites remain only in the direction of this line. This, consequently, leads to the formation of linear *trimers* and eventually linear island chains [see Figs. 1(a) and 2(a)]. Actually, in Fig. 2, the distance between closely "populated" chains is significantly larger than the island distance within such a chain, which probably indicates an independent development of such lines during growth as discussed above.

III. GROWTH SIMULATIONS

A direct kinetic Monte Carlo (KMC) growth simulation is not yet feasible in case of liquid phase epitaxy. Even for MBE KMC cannot treat the three-dimensional growth of arrays of fully developed islands. However, with appropriately chosen growth parameters and a self-consistently included strain field, KMC can simulate the initial stages of MBE growth close to equilibrium conditions until platelets of islands arise.[16,17] With sufficiently long simulations times, the crossover between the initial kinetically controlled regime and thermodynamically limited close-to-equilibrium conditions can also be observed.[18] Therefore it is appropriate to compare our experiments to KMC simulations performed with an anisotropic strain field using the Si/Ge elastic constants.

In the event-based[19] kinetic Monte Carlo scheme we mimic the atomic exchange processes with the liquid phase during epitaxial growth by deposition of atoms and subsequent hopping processes in the growth plane. Equilibration is obtained by a large number of individual hopping events. The probability for a single atom to jump from one lattice position to another is given by an Arrhenius factor

FIG. 3. Atomic force micrographs of $Si_{0.9}Ge_{0.1}$ islands for (a) low and (b) high island coverage. In the vicinity of each island (base width about 1000 nm) the wetting layer thickness is clearly reduced, reproducing well the shape of the elastic energy density (Fig. 4). Note that the height scale has been cut off at 26 nm for reasons of better contrast. The height of the islands is about 500 nm, and the depth of depletion is of the order of 5 nm.
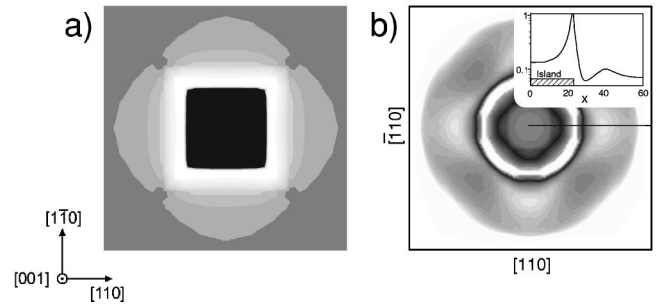
$$p = \nu \exp\{-[E_s + nE_b + E_{str}(x,y)]/(k_B T)\}, \qquad (1)$$

where $\nu = 10^{13}$ s^{-1} is the frequency of attempt, E_s is the surface binding energy of an atom to the wetting layer, E_b is the binding energy to each of the n nearest neighbors, k_B is Boltzmann's constant, and T is the temperature. Atoms can also enter the second growth layer by surmounting a Schwöbel barrier of 0.06 eV at an island edge. In our simulations the binding energies are taken as $E_s = 1.3$ eV and $E_b = 0.3$ eV.[20] Once islands have formed on the surface a strain field is generated around the islands extending about twenty lattice constants away from the island boundary. The strain is responsible for an additional energy term $E_{str}(x,y)$ that influences the motion of adatoms in the vicinity of islands. The local strain field depends on the coordinates $\mathbf{r} = (x,y)$ on the surface, and is calculated self-consistently for the respective island configuration in the context of the continuum theory of elastic media. We use a Green's function formalism[18] to evaluate the elastic displacements $u_i(\mathbf{r})$ by means of the static Green's tensor of elasticity theory $G_{ij}(\mathbf{r},\mathbf{r}')$:

$$u_i(\mathbf{r}) = -\oint_S d^2r' \, G_{ij}(\mathbf{r},\mathbf{r}') P_j(\mathbf{r}'). \qquad (2)$$

The integration is carried out along all island boundaries where the line forces P_j act as the sources of the strain. The strain field is then given by $\varepsilon_{ij}(\mathbf{r}) = \frac{1}{2}(\partial u_i/\partial x_j + \partial u_j/\partial x_i)$.

From this the local elastic strain energy follows as

$$E_{str} = \frac{c_{11}}{2}(\varepsilon_{11}^2 + \varepsilon_{22}^2) + c_{12}\varepsilon_{11}\varepsilon_{22} + 2c_{44}\varepsilon_{12}^2, \qquad (3)$$

where c_{11}, c_{22}, and c_{44} are the elastic constants of a cubic crystal in Voigt notation [Fig. 4(b)]. For group IV semiconductors the $\langle 111 \rangle$ direction (nearest neighbor direction) is the elastically hard direction whereas the $\langle 100 \rangle$ direction is elastically soft, as can be seen in Fig. 4.

In order to simulate close to thermodynamic equilibrium conditions, we choose a low deposition rate of 0.01 monolayers (ML) per second at reasonably high temperatures. Thus we ensure that single adatoms have a long mean free path in comparison to typical island sizes, and island nucleation takes place at energetically favorable positions rather than by accidental dimer formation caused by a large number of diffusing adatoms. We present simulations for a low coverage of $c = 0.05$ [Fig. 1(b)] and a comparatively high coverage of $c = 0.2$ [Fig. 2(b)] on a 400×400 grid, representing a perfect (001) surface. The purpose of our KMC simulations is not to simulate microscopically a specific LPE growth process, but to demonstrate qualitatively the striking feature of island chain formation within a simple growth model. Therefore we do not attempt to match the growth conditions (temperature, growth rate, deposition time, coverage) of experiment and simulation quantitatively. Rather, some plausible ranges of parameters have been chosen in the simulations. In particular, the experimental and the numerical counterparts of Figs. 1 and 2 are typical and do not change much if slightly different coverages or growth rates are used.

For a temperature window from 620 to 700 K we find island chains oriented along $\langle 100 \rangle$ that compare well to the experimental findings (Figs. 1, 2). For low coverage most chains consist of two islands but linear chains containing three or four islands can be found as well. For higher coverage longer chains are formed.

In this temperature regime the islands within the chains tend to have a preferred distance from each other, while the distance beween different chains is larger, exactly as in the experiment (Fig. 2). The centers of mass of two islands in a chain are on average fourteen lattice constants apart. The average island size for a temperature of 650 K is eight lattice constants in diameter. However, the average island size increases with temperature so that for temperatures beyond 700 K islands in the chains begin to cluster.

In comparing Figs. 2(a) and 2(b) one recognizes that in the experiment the island chains exhibit a higher degree of order. The reason for the poorer spatial ordering in the KMC are the large fluctuations present for any finite simulation time. The approach of equilibrium is driven by local variations in the strain field. The equilibrium state is reached by small strain-induced differences in the diffusion constant. The closer the system is to the equilibrium state, the smaller the driving forces become and the slower the approach to equilibrium becomes. Thus a perfect ordering can also be expected for KMC simulations but this would require by orders of magnitude larger computational power.

For very low temperatures the nucleation processes are dominated by random dimer formation and the self-organization of island chains is largely suppressed. Furthermore, for low temperatures the average island size is small resulting in comparatively weak strain fields. Since the spatial ordering is induced by the strain, only little effect can be expected.

Diffusion processes on strained surfaces lead in general to an enhanced mobility of the adatoms caused by the lower binding energy in the strained areas and, as a result, a net current of atoms from the strained regions to the unstrained ones can be observed. Applying these considerations to the material system at hand, one would expect a higher island nucleation rate in the elastically hard directions ($\langle 110 \rangle$) as seen from the island since in those directions the strain decays more rapidly than in the soft directions ($\langle 100 \rangle$), where the strained region extends further away from the island boundary. On the other hand, in the experiment as well as in the computer simulation the island chains are oriented along the soft direction which seems to disprove the above reasoning.

As can be seen in Figs. 4(b) and 5, the elastic anisotropy of the SiGe/Si system generates a monotonically decaying strain field in the soft $\langle 100 \rangle$ direction. In the elastically harder $\langle 110 \rangle$ direction the strain does at first indeed decay faster. There is, however, a local maximum of the strain some distance away from the island boundary that leads to an average flux of adatoms to the areas in the soft direction, where island nucleation is consequently enhanced.

For islands of a size of eight atoms in diameter the local strain maximum in the hard direction is ten lattice constants away from the island boundary. This value agrees well with an average island separation of fourteen lattice constants.
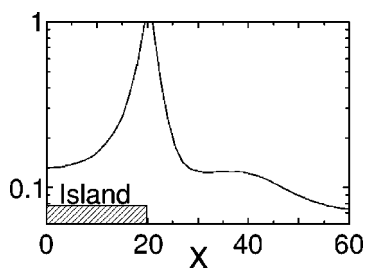
FIG. 5. Strain energy profile of a cut along the soft $\langle 100 \rangle$ direction, taken from Fig. 4(b). (Vertical axis in arbitrary units, x axis in units of the lattice constant.)

IV. CONCLUSIONS

In conclusion, good qualitative agreement between experiment and numerical simulation is found, and a satisfactory understanding of the process of self-organized island chain formation during liquid phase epitaxy has been obtained by our kinetic Monte Carlo simulations, even though this scheme was originally designed for MBE growth. However, it should be noted that under growth conditions close to thermodynamic equilibrium, the large number of individual hopping events simulates well the exchange processes with the liquid phase. It should be kept in mind that we have not attempted to model features which specifically depend upon the LPE growth process and the detailed growth parameters, e.g., the island size (which is in fact in our simulations much smaller than in the experiment, due to the lower growth temperature of our simulations).

Although the growth conditions are close to equilibrium, our kinetic approach has turned out to be appropriate. Of course kinetic effects (diffusion) provide the means of approaching thermodynamic equilibrium. The choice of high temperature and a long equilibration time ensure that a final state close to equilibrium is reached, where kinetic effects are of minor importance and do not limit growth. The virtue of the kinetic Monte Carlo simulations is that they can cover the whole range from the initial purely kinetic regime up to the approach of thermodynamic equilibrium.

[1] D. Bimberg, M. Grundmann, and N. Ledentsov, *Quantum Dot Heterostructures* (John Wiley & Sons, New York, 1999).

[2] I.N. Stranski and L. Krastanow, Akad. Wiss. Lit. Mainz Abh. Math. Naturwiss. Kl. **146**, 797 (1939).

[3] H. Eisele, O. Flebbe, T. Kalka, C. Preinesberger, F. Heinrichsdorff, and A. Krost, Appl. Phys. Lett. **75**, 106 (1999).

[4] K. Zhang, Ch. Heyn, W. Hansen, Th. Schmidt, and J. Falta, Appl. Phys. Lett. **76**, 2229 (2000).

[5] F. Hatami, U. Müller, H. Kissel, K. Braune, R.-P. Blum, S. Rogaschewski, H. Niehus, H. Kirmse, W. Neumann, M. Schmidbauer, R. Köhler, and W.T. Masselink, J. Cryst. Growth **216**, 26 (2000).

[6] Q. Xie, A. Madhukar, P. Chen, and N.P. Kobayashi, Phys. Rev. Lett. **75**, 2542 (1995).

[7] J. Tersoff, C. Teichert, and M.G. Lagally, Phys. Rev. Lett. **76**, 1675 (1996).

[8] V. Holý, G. Springholz, M. Pinczolits, and G. Bauer, Phys. Rev. Lett. **83**, 356 (1999).

[9] D.E. Jesson, G. Chen, K.M. Chen, and S.J. Pennycook, Phys. Rev. Lett. **80**, 5156 (1998).

[10] M. Kästner and B. Voigtländer, Phys. Rev. Lett. **82**, 2745 (1999).

[11] E. Bauser, in *Crystal Growth of Electronic Materials*, edited by E. Kalidis (Elsevier, New York, 1985), p. 41.

[12] M. Schmidbauer, T. Wiebach, H. Raidt, M. Hanke, R. Köhler, and H. Wawra, Phys. Rev. B **58**, 10 523 (1998).

[13] W. Dorsch, H.P. Strunk, H. Wawra, G. Wagner, J. Groenen, and R. Carles, Appl. Phys. Lett. **72**, 179 (1998).

[14] W. Dorsch, B. Steiner, M. Albrecht, H.P. Strunk, H. Wawra, and G. Wagner, J. Cryst. Growth **183**, 305 (1998).

[15] X.Z. Liao, J. Zou, D.J.H. Cockayne, J. Qin, Z.M. Jiang, X. Wang, and R. Leon, Phys. Rev. B **60**, 15 605 (1999).

[16] E. Schöll and S. Bose, Solid-State Electron. **42**, 1587 (1998).

[17] S. Bose and E. Schöll, in *Proceedings of the 24th International Conference on The Physics of Semiconductors (ICPS-24), Jerusalem, Israel*, edited by D. Gershoni (World Scientific, Singapore, 1999).

[18] M. Meixner, R. Kunert, S. Bose, E. Schöll, V.A. Shchukin, D. Bimberg, E. Penev, and P. Kratzer, in *Proceedings of the 25th International Conference on the Physics of Semiconductors (ICPS-25), Osaka 2000*, edited by N. Miura (Springer, Berlin, 2001), p. 381; M. Meixner, E. Schöll, V. A. Shchukin, and D. Bimberg, Phys. Rev. Lett (to be published).

[19] A.B. Bortz, M.H. Kalos, and J.L. Lebowitz, J. Comput. Phys. **17**, 10 (1975).

[20] S. Clarke, M.R. Wilby, and D.D. Vvedensky, Surf. Sci. **255**, 91 (1991).